CORE
Metadata, citation and similar papers at core.ac.uk
Provided by UCL Discovery

TALEN-mediated inactivation of PD-1 in tumor-reactive lymphocytes promotes intratumoral T cell persistence and rejection of established tumors

Running tittle: *Pdcd1* gene inactivation in tumor-reactive lymphocytes

Keywords: checkpoints inhibitors, gene editing, tumor-reactive lymphocytes

PRECIS: This proof of concept study demonstrates that advanced adoptive T cell therapies for cancer can be enhanced by genomic editing strategies to bypass immune checkpoints.

Laurie Menger [1]; Anna Sledzinska [1]; Katharina Bergerhoff [1]; Frederick Arce Vargas [1]; Julianne Smith [2]; Laurent Poirot [2]; Martin Pule [1]; Javier Herrero [1,3]; Karl S. Peggs [1]* and Sergio A. Quezada [1]*

[1]Cancer Immunology Unit, Research Department of Haematology, University College London Cancer Institute, London, UK; [2]Cellectis, Paris, France; [3]Bill Lyons Informatics Centre, University College London Cancer Institute, London, UK.

*K.S.P. and S.A.Q. are co-corresponding authors

Correspondence to:

Sergio A. Quezada, Ph.D and Karl S. Peggs, M.D., Ph.D.
Cancer Immunology Unit
Research Department of Haematology
UCL Cancer Institute
University College London
s.quezada@ucl.ac.uk
karl.peggs@ucl.ac.uk

Competing interests: JS and LP are Cellectis employees.

Abstract

Despite the promising efficacy of adoptive cell therapies (ACT) in melanoma, complete response rates remain relatively low and outcomes in other cancers are less impressive. The immunosuppressive nature of the tumor microenvironment and the expression of immune-inhibitory ligands, such as PD-L1/CD274 by the tumor and stroma are considered key factors limiting efficacy. The addition of checkpoint inhibitors (CPI) to ACT protocols bypasses some mechanisms of immunosuppression, but associated toxicities remain a significant concern. To overcome PD-L1-mediated immunosuppression and reduce CPI-associated toxicities, we used TALEN technology to render tumor-reactive T cells resistant to PD-1 signaling. Here we demonstrate that inactivation of PD-1 in melanoma-reactive CD8+ T cells and in fibrosarcoma-reactive polyclonal T cells enhanced the persistence of PD-1 gene-modified T cells at the tumor site and increased tumor control. These results illustrate the feasibility and potency of approaches incorporating advanced gene-editing technologies into ACT protocols to silence immune checkpoints, as a strategy to overcome locally active immune escape pathways.

Introduction

Adoptive T cell therapy (ACT) using autologous tumor-infiltrating lymphocytes (TILs) or T cells redirected to the tumor by chimeric antigen receptors (CARs) can mediate substantial regression of human cancers (1). Whilst multiple early-phase studies using ACT have demonstrated durable responses which correlate with persistence of the transferred T cells (2, 3), their *in vivo* activity and potency can be thwarted by the complex immunosuppressive nature of the tumor microenvironment (4). Combination protocols incorporating checkpoint inhibitors (CPIs) such as anti-CTLA-4 or anti-PD-L1/PD-1 are currently being considered (NCT02408861; NCT02210117; NCT02374242; NCT02453620) but the potential exacerbation of the toxicities associated with CPIs may limit their implementation. Advanced genetic engineering of the ACT product offers a solution to the toxicity issues by specifically targeting tumor-reactive T cells rather than inducing systemic blockade of the inhibitory checkpoint. The protocols used for the generation of ACT are compatible with genetic manipulation of cells prior to transfer, which can be used to increase the proliferative capacity of lymphocytes (5), to prolong their *in vivo* persistence (6), to improve tumor infiltration (7) as well as to bypass tumor immune suppression.

Programmed Death-1 (PD-1, CD279) is one of the key co-inhibitory immune receptors expressed by activated T cells. Initially described on a T cell hybridoma undergoing cell death (8), PD-1 is a critical regulator of T cell responses and essential to the maintenance of peripheral self-tolerance (9). In mouse and human cancers, high levels of PD-1 are found on TILs, whilst its ligand (PD-L1) is upregulated by tumor and stromal cells in response to inflammatory cytokines (e.g. IFN-γ □ (10, 11). The PDL-1/PD-1 axis plays a major role in tumor growth and immune escape through inhibition of T cell proliferation, effector function (12) and of T cell survival by

promotion of apoptosis (13). The administration of blocking anti-PD-1 or PDL-1 antibodies *in vivo* results in enhanced CD8$^+$ T cell responses and decreases tumor burden in mouse models of cancer (14, 15). In humans, expression of PD-1 by TILs is associated with impaired effector function and/or poor outcome in several tumor types (16, 17). Direct evidence supporting the importance of this pathway in modulating antitumor immunity comes from recent clinical trials in melanoma and non small cell lung cancer, where anti-PD-1 antibodies have improved both progression free and overall survival (18, 19). Of relevance, systemic immunotherapy with CPIs can also induce immune-related adverse events (irAEs). Specific ablation of negative regulators of T-cell function on tumor-reactive T cells used for ACT offers the potential to exploit the antitumor activity whilst reducing systemic toxicity.

Efficient and rapid inactivation of genes in primary antigen-specific T cells is achievable using the transient expression of transcription activator-like effector nucleases (TALEN) mRNA, which offers several safety advantages for clinical applications (20). Using two different mouse models of cancer, we defined the impact of TALEN-mediated PD-1 gene inactivation in adoptively transferred tumor-reactive CD4$^+$ and CD8$^+$ T cells. Our data supports a model in which PD-1 gene inactivation increases persistence of T cells at the tumor site, enhancing tumor control of B16 melanoma by gp-100-reactive CD8$^+$ T cells and mediating complete rejection of established MCA205 fibrosarcoma by endogenous CD4$^+$ and CD8$^+$ T cells. This work demonstrates both the feasibility and the potential potency of strategies incorporating Immune Checkpoint Editing (ICE) of tumor-reactive T cells for use in the context of adoptive T cell therapies for cancer.

Materials and Methods

Mice and cell lines

6- to 8-week-old pmel-1/SJL TCR-transgenic, C57BL/6 and C57BL/6-SJL mice were purchased from Charles River Laboratories Kent. All animal use was in accordance with the Home Office guidelines. The B16.BL6 melanoma cell line was obtained from Prof James Allison, the MCA205 fibrosarcoma cell line was provided by Prof Guido Kroemer, EL4 thymoma cells were provided by Prof Henning Walczak and authentication was performed by the ATCC using short tandem repeat DNA profiles. The cells were grown in RPMI-1640 supplemented with 10% FCS, L-glutamine, Pen/Strept (Sigma-Aldrich).

TALEN construction and validation

Three pairs of TALEN targeting the PD-1 murine gene were produced by Cellectis using the solid phase assembly method (21). Their activity was evaluated in $5x10^6$ EL4 cells, co-transfected with 10 µg of *in vitro* transcribed mRNA (mMESSAGE mMACHINE T7 Kit, Ambion) from each half TALEN (Fig. S1). Three days post transfection, locus specific PCRs were performed on genomic DNA. (Table S1), mutations were assessed by mismatches digestion (T7) and Miseq analysis (20).

Cell culture and adoptive transfer

Splenocytes and lymph nodes cells from pmel-1/SJL transgenic mice were cultured in complete RPMI with gp100 peptide (Pepceuticals) and rhIL-2 (Preprotech) 100UI/mL for 24h prior to selection of $CD8^+$ T cells using Dynabeads FlowComp Mouse CD8 kit. TRL were selected from 100-150mm^3 tumors using Dynabeads FlowComp Mouse Pan T (CD90.2) and maintained in complete RPMI with rhIL-2 (1000UI/mL). $5x10^6$ Pmel-1 $CD8^+$ T cells and MCA205 TRL/180 µL of BTX medium T were mixed with 20 µg of IVT mRNA, prior to electroporation using an Agile Pulse BTX system

(Harvard Apparatus). C57BL/6 mice were subcutaneously implanted with either 2.5×10^5 B16 cells or 4×10^5 MCA205 cells (day 0). On day 6 for the pmel-1 model and on day 4 for the MCA205 model, total body irradiation (TBI) was performed (5 Gy) and 1×10^6 pmel-1 T cells or 1×10^6 MCA205 TRL were adoptively transferred into tumor-bearing mice (n = 5 per group), followed by intraperitoneal (i.p.) injection of rhIL-2 (1.2×10^6 IU) for 3 days. Mice were sacrificed when the tumors exceeded 15 mm in diameter. Mice were treated with the anti-mouse CD8a 2.43 depleting antibody (BioXcell) and the anti-MCH class II M5/114 (BioXcell), i.p. on day 0, 2, 4, 6, 8 after ACT (10 mg/kg).

Flow cytometry

Tumors were weighed, digested in collagenase D (Roche) and mechanically disaggregated through 70-μm filters. Lymph nodes cells and lymphocytes from tumor samples, enriched on a Ficoll gradient were incubated with murine antibodies: anti-CD4-V500 (BD Horizon), anti-CD8-BV650, anti-PD-1-PE-Cy7 (Biolegend), anti-CD45.1-APC-Cy7, anti-FoxP3-AF700, anti-IFN-γ-FITC (re-stimulation with gp100-pulsed dendritic cells for pmel cells or PMA/ionomycin for TRL), anti-KI67-PerCP-eFluor 710, Fixable Viability Dye eFluor 450 (eBioscience), anti-FLICA (Vybrant FAM Poly Caspases Assay Kit, ThermoFisher), annexin-V-PE Apoptosis Detection Kit II (BD Pharmingen), Cell Sorting Set-up Beads (Life Technologies), and anti-human Granzyme B-APC (Invitrogen) in a blocking solution: 5% mouse serum, 5% rat serum (Thermoscientific), 2% FCS, 2% anti-FcR 2.4G2 (BioXcell). Samples were permeabilized using a Fixation/Permeabilization kit (eBioscience), acquired on a LSRII Fortessa and analysed with FlowJo software (Tree-Star).

Western blot analysis

Proteins were separated and subjected to the following antibodies: anti-TALEN

(1mg/ml), anti-GAPDH (D16H11) (Cell signaling, 1:2000), HRP-coupled secondary antibody anti-Rabbit IgG1 HRP-linked (Cell signaling).

Statistical analysis

One-way ANOVA, two-way ANOVA or *t* tests with $P < 0.05$ were performed using Prism 6.0 software (GraphPad). Multiple comparisons were corrected with the Bonferroni coefficient and Kaplan-Meier survival curves were compared with the log-rank test.

For additional information, see supplemental data section

Results and Discussion

TALEN-mediated PD-1 gene inactivation in melanoma reactive $CD8^+$ pmel-1 T cells increases persistence of $CD8^{PD\text{-}1Ex1}$ pmel-1 cells at the tumor site

Three pairs of TALENs targeting the murine PD-1 gene were tested in EL4 cells using an optimized mRNA-electroporation protocol. Only the pair targeting the exon 1 sequence (**Fig. 1A**) caused detectable mismatch-identified mutagenesis (up to 27%) in the PD-1 gene, correlating with loss of PD-1 expression in up to 15% of electroporated EL4 cells (Supplementary **Fig. S1**). To investigate whether PD-1 inactivation of primary tumor-reactive T cells provided superior antitumor activity against the poorly immunogenic mouse melanoma B16 model, we used $CD8^+$ T cell receptor transgenic (TCR Tg) cells specific to the melanoma differentiation antigen gp-100 (pmel-1, Supplementary **Fig. S2A**) (22). *In vitro* activated pmel-1 T cells were electroporated with control GFP mRNA ($CD8^{wt}$) or PD-1-targeting TALEN mRNA ($CD8^{PD\text{-}1Ex1}$), delivering a high transfection efficiency of >85% as confirmed by GFP expression (Supplementary **Fig. S2B**). Western blot analysis confirmed transient TALEN expression one day (d1) after transfection (**Fig.1B**) and Miseq analysis of the targeted sequence showed a high frequency of mutations (53% non-homologous end

joining (NHEJ)) (**Fig. 1C**). Three days after transfection, PD-1 negative cells were enriched using magnetic beads (Supplementary **Fig. S2C**) prior to ACT of $1x10^6$ $CD8^{wt}$ or $CD8^{PD\text{-}1Ex1}$ pmel-1 cells and rhIL-2 into B16 tumor-bearing mice. Significantly enhanced tumor control was consistently observed in mice receiving $CD8^{PD\text{-}1Ex1}$ cells compared to those treated with $CD8^{wt}$ cells (**Fig. 1D**). Six days after transfer *in vivo*, a significant enrichment of tumor-infiltrating PD-1 negative pmel-1 cells was observed in mice treated with $CD8^{PD\text{-}1Ex1}$ T cells (48.2%) (**Fig. 1E upper panel**), which contributed to a 2-fold increase in the total number of tumor-infiltrating pmel-1 cells (**Fig. 1E lower panel**). In contrast,, the absolute number of T cells in draining lymph nodes (DLNs) was similar between the two groups, suggesting that accumulation of $CD8^{PD\text{-}1Ex1}$ T cells at the tumor site was not due to differences in engraftment nor infiltration from the DLNs (Supplementary **Fig. S2D**). Whereas use of RNA and electroporation to deliver TALENs is compatible with future clinical translation, it does not allow incorporation of a reporter gene to distinguish PD-1 edited cells. Nevertheless, the rate of mutagenesis, investigated *ex-vivo* 7 days after ACT demonstrates an effective PD-1 gene editing (70%) in the PD-1 negative fraction from the $CD8^{PD\text{-}1Ex1}$ group (Supplementary **Fig. S2E**). To investigate the mechanisms underpinning enhanced tumor control by pmel-1 cells in the $CD8^{PD\text{-}1Ex1}$ group, we characterized the proliferation and effector functions of $CD8^{wt}$ and $CD8^{PD\text{-}1Ex1}$ T cells in both $PD\text{-}1^+$ and $PD\text{-}1^-$ tumor-infiltrating pmel-1 populations. Contrary to previous work suggesting that PD-1 signaling reduces effector activity at the tumor site (23), no differences were observed in KI67, granzyme B (GZB) or interferon-γ (IFN-γ) expression between $PD\text{-}1^+$ and $PD\text{-}1^-$ cells. When we compared the adjusted percentages (% of cells in $PD\text{-}1^+$ and $PD\text{-}1^-$ sub-populations) of tumor-infiltrating $KI67^+$, GZB^+ and $IFN\text{-}\gamma^+$ cells, we observed that the TALEN-induced PD-1 gene

inactivation did not impact the proliferative or functional characteristics of pmel-1 $CD8^{+}$T cells *in vivo* (Supplementary **Fig. S2F, G, H**). Instead, we consistently observed the appearance of a PD-1^{-} pmel-1 population in the $CD8^{PD\text{-}1Ex1}$ group, which contributed to an increase in the total number of KI67-, GZB- and IFN-γ -expressing cells in tumors from mice receiving $CD8^{PD\text{-}1Ex1}$ T cells (**Fig. 1F, G**). Together these data strongly suggest that, at least in the context of ACT, PD-1 expression primarily controls number of tumor-reactive T cells at the tumor site rather than their proliferative or functional status.

PD-1 gene inactivation of polyclonal tumor-reactive lymphocytes (TRL) promotes persistence of activated $CD4^{+}$ and $CD8^{+}$ at the tumor site

To define the therapeutic potential and functional impact of PD-1 gene inactivation in a more physiologically relevant T cell population, we conducted the PD-1 gene editing of polyclonal tumor-reactive lymphocytes (TRL) from $C57BL/6^{SJL}$ mice, challenged with MCA205 cells (24). $CD4^{+}$ and $CD8^{+}$ T-cells were isolated from the tumor (TILs) and one tumor-draining lymph node (TDLN) via positive selection. After electroporation of the donor TRL, we observed a transfection efficiency >65% and we identified TALEN-induced PD-1 gene mutations by Miseq analysis in 26% of $CD4^{+}$ T cells and almost 40% of $CD8^{+}$ T cells (Supplementary **Fig. S3A, B**).

In parallel to the generation of the donor mock transfected (TRL^{wt}) and PD-1 edited TRL cells ($TRL^{PD\text{-}1Ex1}$), we challenged a separate group of C57BL/6 mice with MCA205 tumors. Four days later, tumor-bearing mice were treated with TBI followed by ACT with TRL^{wt} or $TRL^{PD\text{-}1Ex1}$ cells and rhIL-2. Six days after transfer, analysis of PD-1 expression on TILs from mice receiving TRL^{wt} or $TRL^{PD\text{-}1EX1}$ revealed a 15-20% average increase in PD-1^{-} $CD4^{+}$ and PD-1^{-} $CD8^{+}$ T cells (**Fig. 2A, B**). Consistent with our findings in the TCR Tg model, a significant accumulation of PD-1^{-} cells was

observed only at the tumor site (**Fig. 2C, S3C**). Whilst PD-1 gene inactivation did not alter TRL proliferation (KI67) or function (GZB and IFN-γ) (Supplementary **Fig. S3D, E, F**), the absolute number of PD1^{-} TRL expressing KI67, GZB and IFN-γ was significantly higher in mice receiving TRL$^{PD\text{-}1EX1}$ (**Fig. 2D, E, F**).

Given that the increase in the number of PD-1^{-} cells in mice receiving TRL$^{PD\text{-}1EX1}$ cells was not associated with increased proliferation, we evaluated whether this could be explained by a reduced rate of PD-1-induced death. Using annexin-V and a fluorescent caspase substrate kit (FLICA), we observed an overall reduction in the frequency of intra-tumoral apoptotic cells in PD-1^{-}compared to PD-1^{+} CD4^{+} and CD8^{+} T cells (**Fig. 3A, B, D, E**). Whereas we observed no difference in the frequency of apoptotic cells between mice treated with TRL^{wt} and TRL$^{PD\text{-}1EX1}$, a significant increase in the absolute number of annexin-V^{-} and FLICA^{-} TRL$^{PD\text{-}1EX1}$cells per mg of tumor was reported (**Fig. 3C, F**). The data suggest that instead of increasing T cell reactivity against tumors, TRL$^{PD\text{-}1EX1}$ cells are rendered resistant to PD-1-mediated cell death at the tumor site.

PD-1 gene-inactivation drives CD4 and CD8 dependent rejection of established tumors and long-term memory

PD-1-gene inactivation significantly increased the activity of our ACT protocol (*p=0.0052)* and anti-tumor activity was dependent on both CD8^{+} and CD4^{+} T cells as administration of depleting anti-CD8 or MHC-II blocking antibodies ablated anti-tumor responses (**Fig. 4A, B**). No evidence of tumor recurrence was observed after MCA205 rechallenge on day 50 in mice that had previously rejected tumors (data not shown). The development of long-term memory, as demonstrated by protection against a subsequent tumor challenge, is an important feature of successful T cell adoptive immunotherapy (25). Our data show high levels of KI67, consistent with

high proliferative capacity for both TRL and $TRL^{PD\text{-}1EX1}$ cells, which also displayed a T-bet^{hi} $CD62L^{low}CD44^{hi}$ phenotype consistent with effector memory T cells (Supplementary **Fig. S4A,B**) (27). Finally, *ex-vivo* stimulation of circulating T cells from surviving mice (40 days after tumor rejection) demonstrated high levels of IFN-γ production in both TRL and $TRL^{PD\text{-}1EX1}$ groups arguing against terminal differentiation (Supplementary **Fig. S4C**) (28).

In summary, our data demonstrate the feasibility of application of clinically relevant gene-editing approaches, conferring superior *in vivo* activity in the context of adoptive cell therapy protocols. In both tumor models, mice well tolerated the ACT with no evidence of toxicity (weight, physiological alterations). To the best of our knowledge this is the first proof of concept study illustrating enhancement and persistence of antitumor responses using targeted genome editing of primary tumor reactive T cells. Our data indicate that the primary mechanism by which PD-1 gene inactivation affects tumor-reactive T cells is by regulating their ability to survive rather than increasing their activity on a per cell basis, which aligns with the original description of the role of PD-1 signaling as a pro-apoptotic factor (8). Whilst we investigated PD-1 as the initial proof of concept target, the technology and approach described potentially allows the permanent disruption of one or more other inhibitory checkpoints, conferring a considerable advantage to the design the next generation of cancer immunotherapies.

Authors' Contributions

Conception and design: L. Menger, SA. Quezada, KS. Peggs

Development of methodology: L. Menger

Acquisition of data (provided animals, acquired and managed patients, provided facilities, etc.): L. Menger, A. Sledzinska, K. Bergerhoff, FA. Vargas,

Analysis and interpretation of data (e.g., statistical analysis, biostatistics, computational analysis): L. Menger, A. Sledzinska, J. Herrero

Writing, review, and/or revision of the manuscript: L. Menger, SA. Quezada, KS. Peggs

Administrative, technical, or material support (i.e., reporting or organizing data, constructing databases): L. Menger, J. Smith, L. Poirot

Study supervision: SA. Quezada and KS. Peggs

Grant Support

S.A.Q. is funded by a CRUK Career Development Fellowship and a Cancer Research Institute Investigator Award. K.S.P. receives funding from CRUK, Leukaemia and Lymphoma Research. This work was funded in part by an EU FP7 grant and undertaken at UCL Hospitals/UCL which received support from the Department of Health and CRUK funding schemes for NIH Biomedical Research Centres and Experimental Cancer Medicine Centres.

References and Notes

1. Rosenberg, S. A. and N. P. Restifo "Adoptive cell transfer as personalized immunotherapy for human cancer." *Science* 2015;**348**:62-68.

2. Dudley, M. E., J. R. Wunderlich, P. F. Robbins, J. C. Yang, P. Hwu, D. J. Schwartzentruber, et al. "Cancer regression and autoimmunity in patients after clonal repopulation with antitumor lymphocytes." *Science* 2002;**298**:850-854.

3. Johnson, L. A., R. A. Morgan, M. E. Dudley, L. Cassard, J. C. Yang, M. S. Hughes, et al. "Gene therapy with human and mouse T-cell receptors mediates cancer regression and targets normal tissues expressing cognate antigen." *Blood* 2009;**114**:535-546.

4. Gill, S. and C. H. June "Going viral: chimeric antigen receptor T-cell therapy for hematological malignancies." *Immunol Rev* 2015;**263**:68-89.

5. Liu, K. and S. A. Rosenberg "Transduction of an IL-2 gene into human melanoma-reactive lymphocytes results in their continued growth in the absence of exogenous IL-2 and maintenance of specific antitumor activity." *J Immunol* 2001;**167**:6356-6365.

6. Kalbasi, A., R. K. Shrimali, D. Chinnasamy and S. A. Rosenberg "Prevention of interleukin-2 withdrawal-induced apoptosis in lymphocytes retrovirally cotransduced with genes encoding an antitumor T-cell receptor and an antiapoptotic protein." *J Immunother* 2010;**33**:672-683.

7. Craddock, J. A., A. Lu, A. Bear, M. Pule, M. K. Brenner, C. M. Rooney, et al. "Enhanced tumor trafficking of GD2 chimeric antigen receptor T cells by expression of the chemokine receptor CCR2b." *J Immunother* 2010;**33**:780-788.

8. Ishida, Y., Y. Agata, K. Shibahara and T. Honjo "Induced expression of PD-1, a novel member of the immunoglobulin gene superfamily, upon programmed cell death." *EMBO J* 1992;**11**:3887-3895.

9. Nishimura, H., T. Okazaki, Y. Tanaka, K. Nakatani, M. Hara, A. Matsumori, et al. "Autoimmune dilated cardiomyopathy in PD-1 receptor-deficient mice." *Science* 2001;**291**:319-322.

10. Gros, A., P. F. Robbins, X. Yao, Y. F. Li, S. Turcotte, E. Tran, et al. "PD-1 identifies the patient-specific CD8(+) tumor-reactive repertoire infiltrating human tumors." *J Clin Invest* 2014;**124**:2246-2259.

11. Taube, J. M., R. A. Anders, G. D. Young, H. Xu, R. Sharma, T. L. McMiller, et al. "Colocalization of inflammatory response with B7-h1 expression in human melanocytic lesions supports an adaptive resistance mechanism of immune escape." *Sci Transl Med* 2012;**4**:127ra137.

12. Tseng, S. Y., M. Otsuji, K. Gorski, X. Huang, J. E. Slansky, S. I. Pai, et al. "B7-DC, a new dendritic cell molecule with potent costimulatory properties for T cells." *J Exp Med* 2001;**193**:839-846.

13. Dong, H., S. E. Strome, D. R. Salomao, H. Tamura, F. Hirano, D. B. Flies, et al. "Tumor-associated B7-H1 promotes T-cell apoptosis: a potential mechanism of immune evasion." *Nat Med* 2002;**8**:793-800.

14. Blank, C., I. Brown, A. C. Peterson, M. Spiotto, Y. Iwai, T. Honjo, et al. "PD-L1/B7H-1 inhibits the effector phase of tumor rejection by T cell receptor (TCR) transgenic CD8+ T cells." *Cancer Res* 2004;**64**:1140-1145.

15. Barber, D. L., E. J. Wherry, D. Masopust, B. Zhu, J. P. Allison, A. H. Sharpe, et al. "Restoring function in exhausted CD8 T cells during chronic viral infection." *Nature* 2006;**439**:682-687.

16. Thompson, R. H., H. Dong, C. M. Lohse, B. C. Leibovich, M. L. Blute, J. C. Cheville, et al. "PD-1 is expressed by tumor-infiltrating immune cells and is associated with poor outcome for patients with renal cell carcinoma." *Clin Cancer Res* 2007;**13**:1757-1761.

17. Ahmadzadeh, M., L. A. Johnson, B. Heemskerk, J. R. Wunderlich, M. E. Dudley, D. E. White, et al. "Tumor antigen-specific CD8 T cells infiltrating the tumor express high levels of PD-1 and are functionally impaired." *Blood* 2009;**114**:1537-1544.

18. Robert, C., J. Schachter, G. V. Long, A. Arance, J. J. Grob, L. Mortier, et al. "Pembrolizumab versus Ipilimumab in Advanced Melanoma." *N Engl J Med* 2015;**372**:2521-2532.

19. Brahmer, J., K. L. Reckamp, P. Baas, L. Crino, W. E. Eberhardt, E. Poddubskaya, et al. "Nivolumab versus Docetaxel in Advanced Squamous-Cell Non-Small-Cell Lung Cancer." *N Engl J Med* 2015;**373**:123-135.

20. Menger, L., A. Gouble, M. A. Marzolini, A. Pachnio, K. Bergerhoff, J. Y. Henry, et al. "TALEN-mediated genetic inactivation of the glucocorticoid receptor in cytomegalovirus-specific T cells." *Blood* 2015;**126**:2781-2789.

21. Daboussi, F., S. Leduc, A. Marechal, G. Dubois, V. Guyot, C. Perez-Michaut, et al. "Genome engineering empowers the diatom Phaeodactylum tricornutum for biotechnology." *Nat Commun* 2014;**5**:3831.

22. Overwijk, W. W., A. Tsung, K. R. Irvine, M. R. Parkhurst, T. J. Goletz, K. Tsung, et al. "gp100/pmel 17 is a murine tumor rejection antigen: induction of "self"-reactive, tumoricidal T cells using high-affinity, altered peptide ligand." *J Exp Med* 1998;**188**:277-286.

23. Keir, M. E., M. J. Butte, G. J. Freeman and A. H. Sharpe "PD-1 and its ligands in tolerance and immunity." *Annu Rev Immunol* 2008;**26**:677-704.

24. Kjaergaard, J. and S. Shu "Tumor infiltration by adoptively transferred T cells is independent of immunologic specificity but requires down-regulation of L-selectin expression." *J Immunol* 1999;**163**:751-759.

25. Wang, L. X., J. Kjaergaard, P. A. Cohen, S. Shu and G. E. Plautz "Memory T cells originate from adoptively transferred effectors and reconstituting host cells after sequential lymphodepletion and adoptive immunotherapy." *J Immunol* 2004;**172**:3462-3468.

26. Odorizzi, P. M., K. E. Pauken, M. A. Paley, A. Sharpe and E. J. Wherry "Genetic absence of PD-1 promotes accumulation of terminally differentiated exhausted CD8+ T cells." *J Exp Med* 2015;**212**:1125-1137.

27. Seder, R. A. and R. Ahmed "Similarities and differences in CD4+ and CD8+ effector and memory T cell generation." *Nat Immunol* 2003;**4**:835-842.

28. Paley, M. A., D. C. Kroy, P. M. Odorizzi, J. B. Johnnidis, D. V. Dolfi, B. E. Barnett, et al. "Progenitor and terminal subsets of CD8+ T cells cooperate to contain chronic viral infection." *Science* 2012;**338**:1220-1225.

29. Yao, S. and L. Chen "Reviving exhausted T lymphocytes during chronic virus infection by B7-H1 blockade." *Trends Mol Med* 2006;**12**:244-246.

Figure legends

Fig. 1: TALEN-mediated PD-1 gene inactivation in pmel-1 $CD8^{+}$T cells enhances the antitumor activity of ACT. (**A**) Schematic representation of murine *Pdcd1* gene (chr. 1) and TALEN targeted sequence (exon 1). (**B**) TALEN protein expression at day 1, 2, 3 after transfection. (**C**) TALEN-induced mutagenesis (>50%) by Miseq analysis of $CD8^{PD\text{-}1Ex1}$ pmel-1 T cells. NHEJ: non-homologous end joining. (**D**) B16 tumor growth curve in mice receiving $1x10^{6}$ $CD8^{wt}$ cells or $CD8^{PD\text{-}1Ex1}$ ACT, 6 days after tumor challenge. (**E**) PD-1 expression on tumor-infiltrating $CD8^{+}$ T cells and transferred cells engraftment at the tumor site. (**F, G**) Proliferation (KI67) and functional analysis of tumor-infiltrating $CD8^{wt}$ cells or $CD8^{PD\text{-}1Ex1}$ depicting GZB and IFN-γ expressions. Each dot represents an individual mouse, and histograms represent mean ± SD of 2 independent experiments (n=10), two-way ANOVA ($^{**}P<0.01$; $^{***}P<0.001$).

Fig. 2: Functional analysis of ACT with PD-1 gene inactivation on TRL 6 days after transfer *in vivo*. (**A**) Flow plots depicting PD-1 expression on TRL^{wt} or $TRL^{PD\text{-}1\text{-}Ex1}$ T cells. (**B**) Percentage of $PD\text{-}1^{-}$ cells showing an average of 15-20% increase on $TRL^{PD\text{-}1\text{-}Ex1}$ compared to TRL^{wt} T cells. (**C**) Absolute number of $PD1^{+}$ and $PD1^{-}$ TRL^{wt} and $TRL^{PD\text{-}1\text{-}Ex1}$ T cells per mg of tumor. (**D**, **E, F**) Representative flow plots showing KI67-, GZB- and IFN-γ-expressions on $CD4^{+}$ and $CD8^{+}$ TRL^{wt} and $TRL^{PD\text{-}1\text{-}Ex1}$ T cells and absolute number of cells per mg of tumor. Each dot plot represents an individual mouse, and histograms represent mean ± SD of 3 independent experiments (n=15). Non-parametric *t* test (B), two-way ANOVA (C, E, F) $^{*}P<0.05$, $^{**}P<0.01$, $^{***}P<0.001$.

Fig. 3: PD-1 regulates the survival of adoptively transferred TRL *in vivo*. (**A, D**) Representative histograms depicting the annexin-V/FLICA positivity in $PD\text{-}1^{+}$ and $PD\text{-}1^{-}$ TRL 6 days after ACT. (**B, E**) Adjusted percentage of annexin-V^{+}/$FLICA^{+}$

cells in PD-1^+ and PD-1^- subsets of $CD4^+$ and $CD8^+$ TRL^{wt} and $TRL^{PD\text{-}1Ex1}$T cells. Histograms represent mean ± SD from 2 independent experiments (n=10). (**C, F**) Absolute numbers of annexin-V^-/$FLICA^-$ $CD4^+$ and $CD8^+$ TRL per mg of tumor. Two-way ANOVA (B), and multiple comparison one-way ANOVA with Bonferroni correction (C) $^{**}P<0.01$, $^{***}P<0.001$.

Fig. 4: Therapeutic efficacy of ACT with PD-1 gene inactivation of TRL on MCA205 fibrosarcoma. (**A**) MCA205 growth curve after ACT with TRL and CD8 depleting or MHC-II blockade antibodies. Two-way ANOVA $^{*}P<0.05$, $^{**}P<0.01$. (**B**) Treatment with $TRL^{PD\text{-}1Ex1}$ resulted in significant prolongation of survival (n=15). Log-rank test, P=0.0052. Depletion of $CD8^+$ subset or MHC-II blockade abrogates the $TRL^{PD\text{-}1Ex1}$ cells–induced antitumor effects (n=10).

Fig. 1

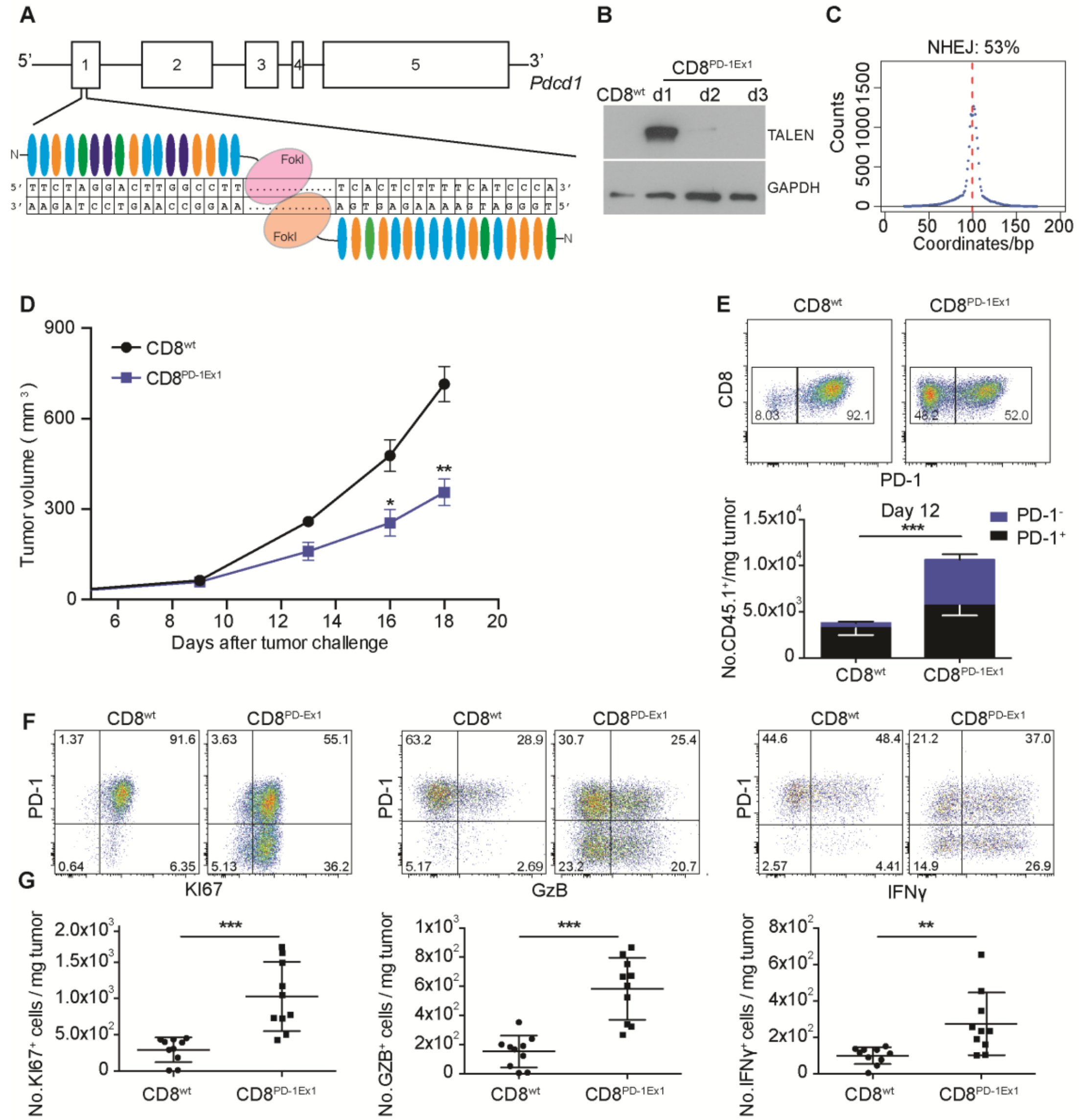

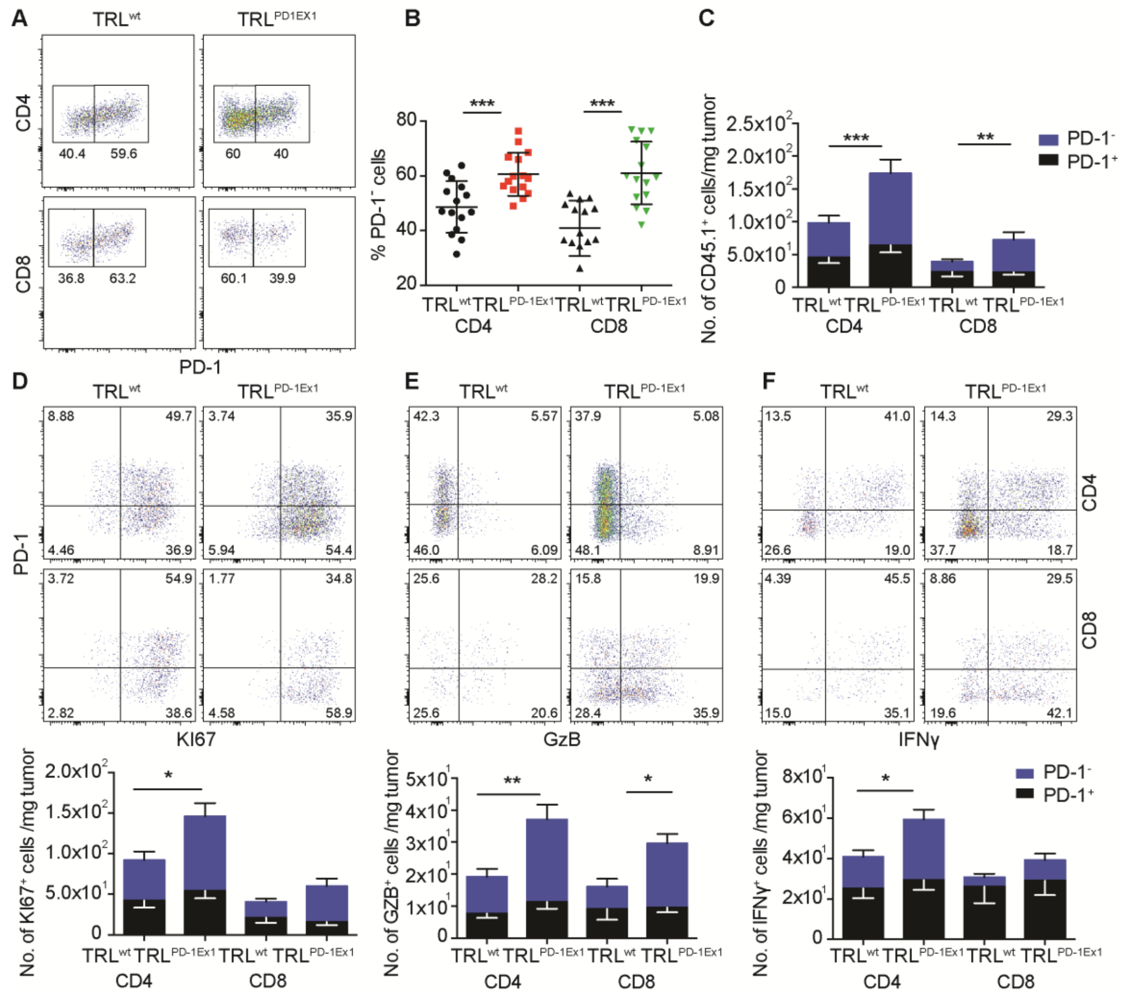
Fig.2
A
B
C
D
E
F
TRL^wt
TRL^PD1EX1
TRL^PD-1Ex1
CD4
CD8
PD-1
% PD-1⁻ cells
No. of CD45.1⁺ cells/mg tumor
PD-1⁻
PD-1⁺
KI67
GzB
IFNγ
No. of KI67⁺ cells /mg tumor
No. of GZB⁺ cells /mg tumor
No. of IFNγ⁺ cells /mg tumor

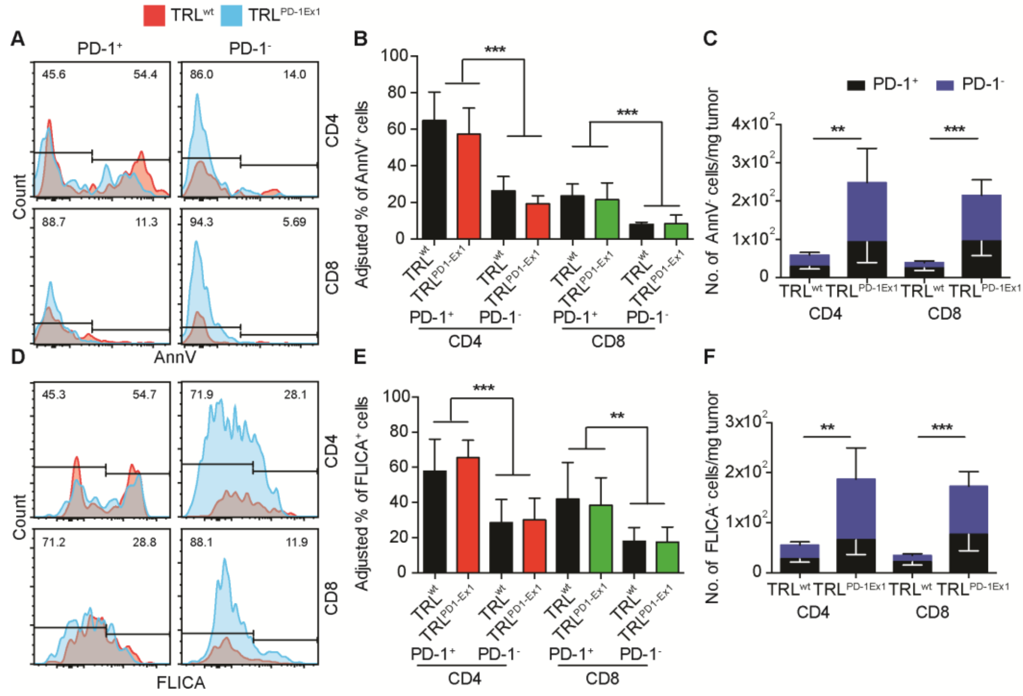
Fig.3
TRLwt
TRLPD-1Ex1
A
PD-1+
PD-1-
B
C
PD-1+
PD-1-
CD4
CD8
Count
AnnV
Adjusted % of AnnV+ cells
No. of AnnV- cells/mg tumor
D
E
F
FLICA
Adjusted % of FLICA+ cells
No. of FLICA- cells/mg tumor

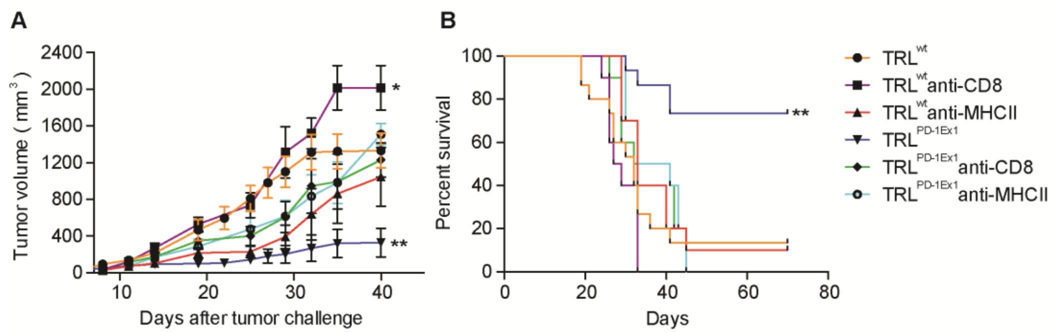
Fig. 4
A
B
Tumor volume (mm3)
Days after tumor challenge
Percent survival
Days
TRLwt
TRLwtanti-CD8
TRLwtanti-MHCII
TRLPD-1Ex1
TRLPD-1Ex1anti-CD8
TRLPD-1Ex1anti-MHCII